Measurements of isobaric VLL equilibria of the 1,1,4,4-tetramethyl-2-tetrazene-water binary system: novel experimental approach and modeling essays

Anne-Julie Bougrine, Anne Renault, Marie-Rose Frangieh, Chaza Darwich

Measurements of isobaric VLL equilibria of the 1,1,4,4-Tetramethyl-2-tetrazene - Water binary system: novel experimental approach and modelling essays

*Anne-Julie Bougrine, Anne Renault, Marie-Rose Frangieh and Chaza Darwich**

Univ Lyon, Univ Claude Bernard Lyon 1, CNRS, CNES, ArianeGroup, LHCEP, UMR 5278 Bât. Raulin, 2 rue Victor Grignard, F-69622 Villeurbanne, France

* **Corresponding Author**

E-mail: chaza.darwich@univ-lyon1.fr

ORCID

Chaza Darwich: 0000-0003-2332-8132

KEYWORDS: tetramethyltetrazene, LLV equilibria, heteroazeotrope, DSC, continuous process

ABSTRACT: The present study was carried out in the frame of the optimization of the synthesis process of 1,1,4,4-tetramethyl-2-tetrazene (TMTZ), a prospective liquid propellant. The liquid-liquid (LL) equilibria of the TMTZ + H_2O binary system were studied under atmospheric pressure and in the range of temperature from 278.15 up to 348.15 K. These results established the conditions leading to a spontaneous demixing of TMTZ from the aqueous synthesis solutions. The experimental study of the liquid-vapor (VL) equilibria of the TMTZ + H_2O system by DSC, under atmospheric pressure, highlighted the various equilibrium domains involved in the distillation step. Lastly, the thermodynamic modelling of those equilibria, using various models (Van Laar, NRTL, Wilson), enabled to refine the experimental results in order to enhance the extraction conditions leading to the production of ultra-pure TMTZ.

1. INTRODUCTION

Hydrazines are liquid reductants particularly suited for space applications. They can either be used as monopropellants in trajectory correction thrusters or as bi-propellants, associated with strong oxidizers such as white or red fuming nitric acid or nitrogen tetroxide. In particular, monomethylhydrazine is nowadays the most widely used storable propellant. Indeed, it can be used in launch vehicles, satcoms, motion correction motors, space shuttles and in the International Space Station ISS refueling vehicle [1-5]. Unfortunately, the former compounds have registered CMR (Carcinogenic, Mutagenic and Reprotoxic) activity and are highly toxic. Additionally, they are volatile and might form explosive mixtures with air [6]. The ECHA (European Chemical Agency) has listed hydrazines as Substances of Very High Concern (SVHC) and the REACH (Registration, Evaluation, Authorization and restriction of CHemicals) European Union regulation has set out to ban them in the short to mid-term [7-10]. It is therefore imperative to find alternative compounds to replace hydrazines. In this context, our laboratory has developed a polynitrogenated derivative that can be a plausible susbtitute for hydrazines in rocket propulsion. Indeed, a study describing a new synthesis and extraction process of 1,1,4,4-tetramethyl-2-tetrazene (TMTZ) and featuring his properties has been already reported [11]. TMTZ can be considered as an interesting candidate due to its several advantages : a) its theoretical performances are comparable to hydrazines, b) its vapor pressure is lower than hydrazines (i.e., limits the risk of exposure through inhalation), c) it is less toxic than hydrazines, d) it is a hypergolic fuel, e) it is liquid in a large temperature domain, between 248.15 and 423.15 K (i.e., no major change in the rocket architecture) and f) its synthesis is suitable for large scale continuous production.

This synthesis and extraction process presents a cleaner and scalable alternative to the previously reported methods based on the use of toxic, unstable or expensive oxidants such as silver oxide, mercury oxide, halides or selenium oxide [12]. It uses monochloramine as oxidant of unsymmetrical dimethylhydrazine (UDMH), and have the following advantages: a) it uses available and affordable starting materials, as monochloramine is prepared *in situ* from sodium hypochlorite and ammonia solution and it does not require any further purification before its reaction on UDMH, b) all synthesis steps are carried out in aqueous solution, with no use of expensive or toxic solvent, c) ammonium chloride, the main by-product, is non-polluting and easily recyclable, d) the extraction process can be facilitated by a spontaneous phase separation of TMTZ with a purity of 90-95 %, e) the yields obtained are between 80 and 90 %, f) the possibility of UDMH recycling according to the flowsheet representing the optimized process (Figure 1). The synthesis parameters of this process have been already optimized thanks to a kinetic and mechanistic study of the various reactions occurring along the formation of TMTZ [11].

Considering the optimum conditions for synthesis and extraction, the TMTZ production process includes the following steps (Figure 1):

1. Preparation of a solution of monochloramine at 1 $mol.L^{-1}$ by the action of sodium hypochlorite on an ammonia solution at low temperature (yield > 95%).
2. Alkalinization of the chloramine solution to ensure a sodium hydroxide concentration of 0.3 $mol.L^{-1}$ at the end of the next step.
3. Synthesis of dimethylhydrazine by addition of the monochloramine obtained at step 1 to an excess of dimethylamine DMA, optimally equal to 8 (yield = 93%).
4. Stripping of ammonia and dimethylamine, then separation of these two reagents in excess for an upstream recycling.
5. Distillation of UDMH from its synthesis medium under reduced pressure, leading to a 99% pure compound.
6. Acidification of the UDMH solution by adding an aqueous solution of hydrochloric acid to obtain a pH of 8.
7. Synthesis of TMTZ by oxidation of UDMH, either in anhydrous form or in situ, in its synthetic medium, with the chloramine solution resulting from step 1. The UDMH / monochloramine molar ratio is preferably equal to 4 and the reactor temperature is around 288.15 K.
8. Spontaneous demixing of the medium, leading to quite pure TMTZ (purity > 95 %) in the upper phase. The lower aqueous phase contains predominantly water, NaCl, NH_4Cl and the excess of UDMH.
9. Distillation of the organic phase under reduced pressure, enabling to collect TMTZ with a purity higher than 99 %.

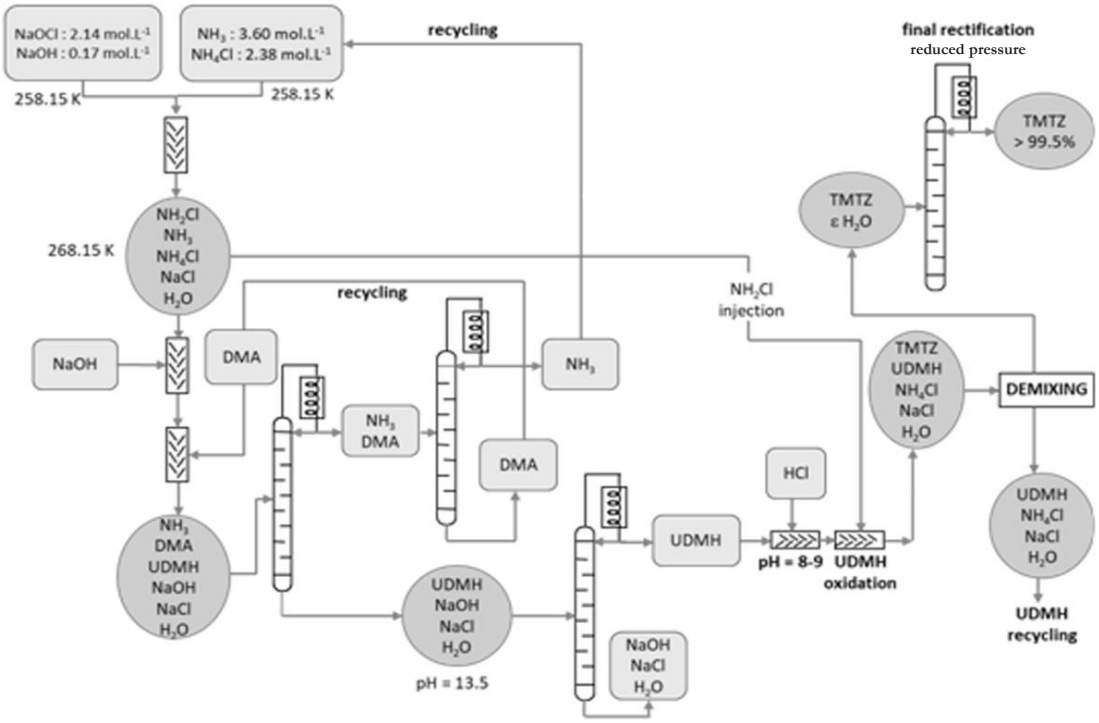

Figure 1 Flowsheet of the continuous production process of TMTZ obtained from UDMH oxidation using monochloramine

In order to support the abovementioned published work and to complement the extraction data of this flowsheet, we describe herein a study aiming to optimize the extraction steps of the TMTZ production process. The present thermodynamic investigation involves first the study of the LL equilibria of the TMTZ + H_2O binary system in order to refine the conditions leading to the spontaneous demixing of TMTZ from the aqueous synthesis solutions. As the extraction process includes a final distillation step, the second part of this study involves defining the corresponding optimal conditions, which requires the characterization of the VL equilibria of the TMTZ + H_2O binary system. Moreover, a third part is dedicated to the modelling of the VL equilibria to complement the experimental data and to explore the domains, which are difficult to reach experimentally.

2. EXPERIMENTAL SECTION

2.1. Products

The TMTZ samples were synthesized and purified by distillation [11], they all had a purity superior to 99.8 %. The properties of this compound are given in Table 1. Demineralized water, used for LL equilibria samples, DSC (Differential Scanning Calorimetry) samples and for the preparation of titrating solutions was obtained from city water by passage through an ion exchange resin (Aquadem from Veolia Water).

Table 1. Main properties of tetramethyltetrazene (TMTZ)

IUPAC Name	Molecular Formula	Molecular Weight /g·mol^{-1}	Final Mass Fraction Purity	Purification Method	Analysis Method	Structural Formula
N-[(E)-dimethylaminodiazenyl]-N-methylmethanamine	$C_4H_{12}N_4$	116.168	> 0.998	distillation	GC	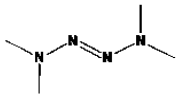

2.2. Methods and apparatus

The LL equilibria were studied in a 100 mL double-jacketed separation funnel. The device was thermostatically controlled by a cryothermostat HMT 200 from HETO, enabling the temperature control with a precision of 0.1 K. A series of 50 mL binary mixtures TMTZ + H_2O, of circa 50 % initial weight composition were prepared. The acid-base titrations were carried out on a TitrinoPlus 848 titrator from Metrohm, using a combined pH glass electrode (Metrohm AG 9101). The water content of the organic phases was determined on a Karl Fisher coulometric titrator C20 from Mettler, using the Hydranal Coulomat AG reagent.

The vapor pressure of TMTZ was determined using a static device dedicated to low vapor pressure measurements [13-15]. The instrument was calibrated with naphtalene.

The DSC measurements were carried out on a DSC 131 from Setaram. The calorimeter was calibrated using standards of Indium (T^0_{fus} = 429.75 K), Tin (T^0_{fus} = 505.09 K) and Lead (T^0_{fus} = 600.62 K).

Samples of TMTZ + H_2O binary mixtures were prepared, covering the entire range of TMTZ composition from 0 to 100 %w. A suitable mass of each component, calculated to obtain the desired mass fraction, was weighed on a ± 0.1 mg precision analytical balance (Mettler ME204). A total mass of circa 10 mg of the prepared mixture was introduced in unpierced lid Aluminum crucible. The mixtures were analyzed by DSC in the temperature range 293.15 - 423.15 K, using a temperature ramp of 3 K / min.

3. EXPERIMENTAL RESULTS

3.1. Determination of the LL equilibria

One at time, the mixtures were introduced into the funnel, well shaken and brought to the set temperature thanks to the cryothermostat. Over a temperature range between 278.15 and 348.15 K, biphasic mixtures have been systematically obtained. They were decanted for three hours at the set temperature and under atmospheric pressure. After three hours, the system reached its equilibrium as no more evolution were observed for the compositions of the two liquid phases. The mixture temperature was then accurately measured by means of a thermometer, and a sampling of each phase was collected. The funnel being an open environment, pressure value is the normal atmospheric pressure. The TMTZ concentration in the aqueous phase was determined by an acid-base dosage, using a 0.1 N HCl titrating solution. The water content of the TMTZ phase was measured by the Karl Fisher method.

The mass and molar compositions of TMTZ in the aqueous and organic phases are reported in Table 2. Concentrations uncertainties were determined thanks to replicated experiments. The results obtained showed a very low regressive solubility of TMTZ in water, ranging from 5 to 1.8 %w at temperatures ranging from 278.15 up to 348.15 K. In addition, the water content of the TMTZ phases is less than 1.2 %w in the abovementioned temperature range. These results confirmed the spontaneous demixing of TMTZ from its synthesis medium.

Table 2. Experimental (Liquid + Liquid) Molar Fractions *x* and Mass Fractions *w* for {Tetramethyltetrazene (1) + Water (2)} binary system as a Function of Temperature *T* and Pressure *p* = 101.33 kPa

T^a/K	Aqueous phase		Organic phase	
	$100 \cdot w_1{}^a$	$x_1{}^a$	$100.w_1{}^a$	$x_1{}^a$
278.9	4.9	0.008	99.5	0.971
283.8	3.4	0.005	99.5	0.966
289.2	2.8	0.004	99.4	0.965
294.9	2.4	0.004	99.4	0.964
298.1	2.3	0.004	99.5	0.971
304.0	2.1	0.003	99.5	0.966
308.8	2.0	0.003	99.4	0.962
325.2	2.3	0.004	99.1	0.943
332.2	2.1	0.003	98.9	0.934

338.2	2.6	0.004	98.8	0.929
347.2	1.8	0.003	99.0	0.940

[a] Standard uncertainties are: $u(p)$ = 10 kPa, $u(T)$ = 0.1 K, $u(100 \cdot w)$ = 0.2, $u(x)$ = 0.002.

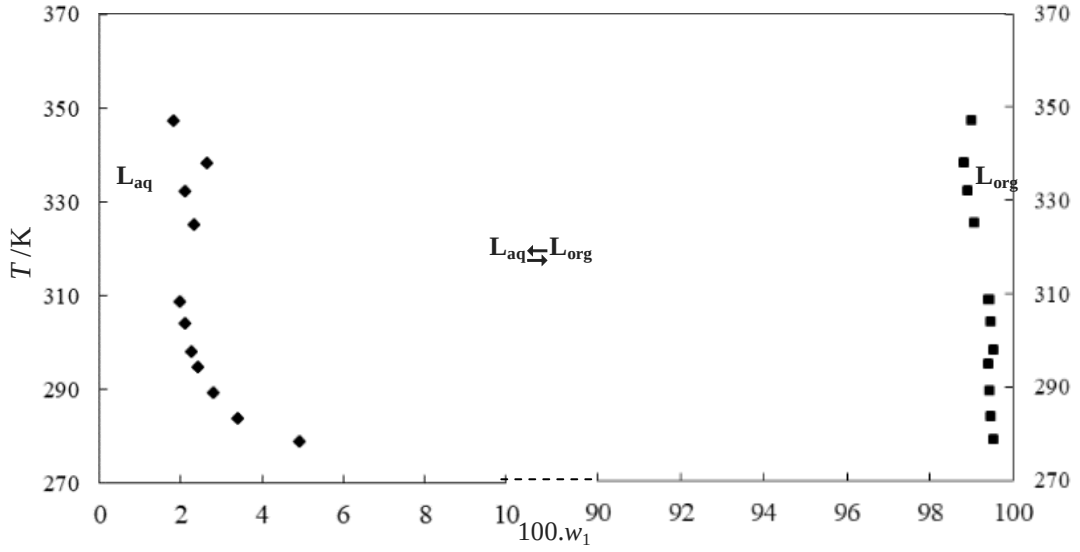

Figure 2 Experimental LLE data for the {Tetramethyltetrazene (1) + Water (2)} binary system, p = 101.33 kPa ◆ : aqueous liquid; ■ : organic liquid

The plot of the LL phase diagram TMTZ + H_2O (Figure 2) shows solubility curves parallel to the temperature axis, suggesting that the two compounds are immiscible up to their vaporization temperatures. This immiscibility was predictable due to the differences in polarity and chemical structure between the two pure compounds.

3.2. Determination of the vapor pressure of TMTZ

The vapor pressure of TMTZ was measured as a function of temperature, using a static instrument dedicated to low vapor pressure measurements, in the range 0.133 - $37.33 \cdot 10^3$ Pa [13-15]. The experimental data are reported in Table 3.

Table 3. Experimental and Calculated Data for TMTZ Vapor Pressures p_s as Function of Temperature T [Relative Deviation $\Delta p = |(p_{calc} - p_{exp})/p_{exp}|$]

T [a] /K	p_s [a] exp /Pa	p_s calc /Pa	Δp /Pa
273.1	228	228	0.000

283.1	460	461	0.002
293.2	875	880	0.006
303.2	1607	1601	0.004
313.2	2797	2779	0.006
323.2	4650	4633	0.004
333.2	7440	7454	0.002
343.2	11548	11620	0.006
353.2	17445	17605	0.009
363.2	26237	25971	0.01

[a] Standard uncertainties are: $u(T) = 0.2$ K, $u(p) = 0.01 \cdot k$Pa.

The adjustment of the experimental results enabled to deduce the parameters of the Antoine equation (Table 4). These results showed a good match between experimental and calculated saturation vapor pressures, with only 0.5 % as deviation. The conformity of the experimental data with the theory validated the obtained results (Figure 3).

Table 4. Adjustment of the Antoine's equation parameters

Antoine equation	$\log(p) = A - B/(C+T)$	p /Pa, T /K	T = (273.15 to 363.15) K
Parameters	Uncertainties on the **Antoine's equation** parameters	Standard deviation	Uncertainty on p
A = 9.59 B = 1641 K C = - 46 K	ΔA = 0.09 ΔB = 50 K ΔC = 4 K	$\lvert\Delta p\rvert_{moy}$ = 56 Pa	$\left\lvert\frac{\Delta p}{p}\right\rvert_{moy}$ = 0.49 %

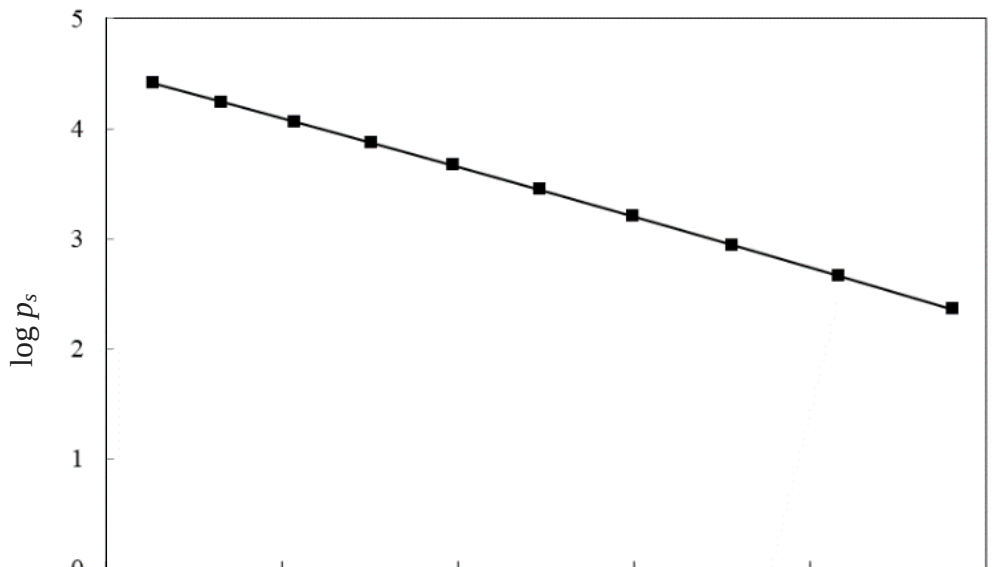

Figure 3 Saturation vapor pressures of TMTZ as function of 1/*T* and correlation with the Antoine equation ■: this work; ─: calculated data

3.3. Determination of the LLV equilibria of the TMTZ-H_2O binary system

First, the TMTZ + H_2O binary system was studied by ebulliometry under reduced pressure. However, whatever the initial composition of the mixture, the equilibrium temperature remained the same. Those results were elucidated, taking into account the fact that, when the equilibrium of the system is reached, three phases are present and the variance of the system is equal to zero. The temperature of the heteroazeotrope is therefore constant. As a matter of fact, the design of the ebulliometry device does not allow for reaching temperature domains beyond the invariant plateau.

Indeed, since the system operates in a closed loop, each biphasic mixture, when it reaches its boiling point, has the temperature of the heteroazeotropic plateau and the phases in equilibrium have the same composition in each case. This method therefore only enabled the determination of the heteroazeotrope temperature but gave no result concerning the phase compositions (T_H = 324 ± 1 K; $p = 17 \cdot 10^3$ Pa).

An alternative was therefore explored to study this system. DSC is a commonly used technique for determining the solid-liquid transitions of organic and inorganic compounds. It is very suitable for the study of melting temperature and enthalpy measurements. More rarely, it can also be used to characterize LV equilibrium from the onset temperature of the endothermic peak corresponding to the vaporization [16-17]. Moreover, methods have been recently developed for the determination of vaporization phenomena of binary mixtures [18].

The TMTZ + H_2O system was studied by DSC at the atmospheric pressure. First of all, a series of preliminary tests was carried out in order to determine the optimal conditions (sample mass, crucible and lid, crucible volume) enabling to visualize the vaporization at the desired pressure without loss of the sample.

TMTZ + H_2O mixtures were analyzed using 120 μL aluminum crucibles equipped with unpierced lids. The heating rate was adjusted so as to find the best compromise between an optimal separation of the peaks and the absence of pre-evaporation of the constituents before reaching the equilibrium temperature.

The optimal conditions were observed in the course of heating using a temperature ramp of 3 K / min, in the range 293.15 - 423.15 K. For each binary mixture, the thermograms showed two endothermic peaks, more or less deconvoluted depending on the initial composition of the mixture (Figure 4). The first peak corresponds to the vaporization of the heteroazeotrope, and the second peak to the vaporization of the remaining liquid phase. The crucibles are not sealed, so, we assumed that the working pressure was around the normal atmospheric pressure (no pressure device around the crucibles).

For each thermogram, the onset temperatures of each peak were determined by plotting the intersection between the tangent of the endothermic peak and the baseline (Table 5). Uncertainties for vaporization temperatures and enthalpies were determined thanks to replicated experiments.

The scattering of the experimental data of the heteroazeotropic invariant temperature is related to the measurement uncertainties.

Table 5. Experimental Thermodynamic Data of the DSC Thermograms (Vaporization Temperature T_{vap} and Enthalpies ΔH_{vap}) Recorded for {TMTZ (1) + H_2O (2)} binary mixtures as a Function of the Mass Fractions w_1

	Heteroazeotrope		Vaporization	
$100.w_1$[a]	$T_{vap}{}^a$ /K	$\Delta_{vap}H^a$ /J·g^{-1}	$T_{vap}{}^a$ /K	$\Delta_{vap}H^a$ /J·g^{-1}
0.0	-	-	373.1	2258
11.4	364.3	46	374.0	1871
13.2	364.0	75	373.0	1950
23.8	364.7	299	372.9	1425
28.4	364.4	374	372.4	1333
40.3	365.4	492	371.7	854
42.3	367.1	481	371.1	756
45.3	365.8	524	371.1	821
50.7	365.8	642	370.6	588
52.4	365.7	829	371.6	276
53.9	366.4	706	371.0	464
55.7	366.8	742	370.8	480
58.4	366.0	740	370.4	392
60.2	366.2	711	371.2	354
61.3	366.6	768	370.2	228
61.6	366.0	796	370.9	259

63.6	366.3	831	370.5	199
66.0	366.3	875	374.3	56
73.3	367.7	773	392.2	14
74.0	367.6	763	395.5	25
75.2	367.7	735	394.7	34
78.9	365.3	630	395.9	67
85.0	365.6	477	397.5	104
92.2	-	-	397.9	85
100.0	-	-	400.1	267

[a] Standard uncertainties are: $u(100 \cdot w) = 0.2$ %, $u(T) = 0.6$ K, $u(\Delta_{vap}H) = 0.05 \cdot \Delta_{vap}H$ J·g^{-1}.

$100 \cdot w_1$	11.4	50.7	58.4	78.9

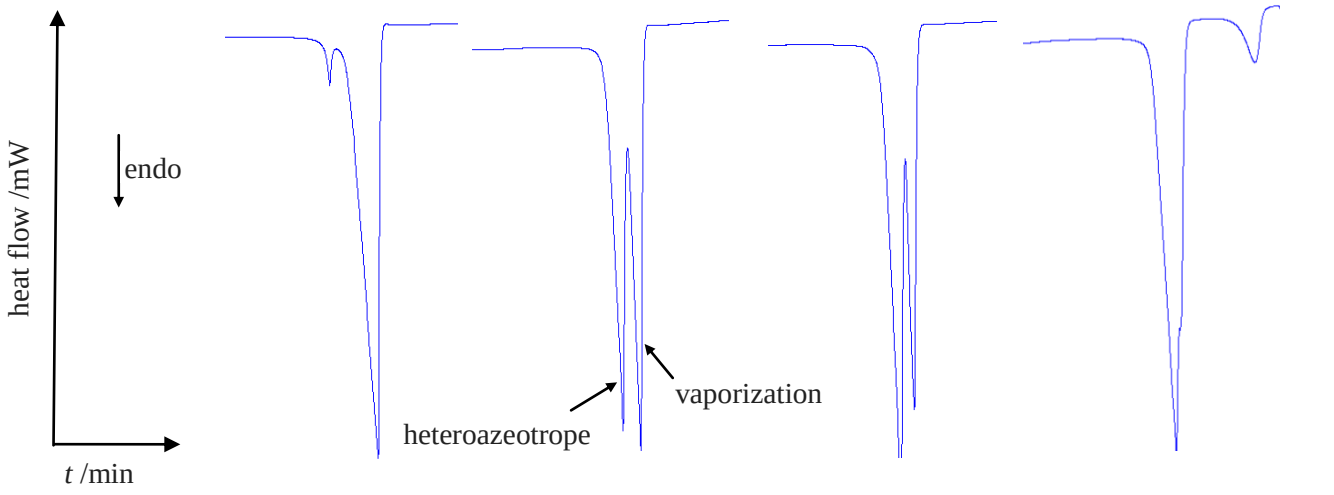

Figure 4 DSC Thermograms of the {Tetramethyltetrazene (1) + Water (2)} binary mixtures (%w_1 = 11 to 85 %; 3 K·min^{-1}; 120 μL Al crucibles)

Figure 5 represents the TMTZ + H_2O VLL diagram, including the following domains:

- one demixing domain L_{aq} + L_{org},
- two monophasic liquid domains,
- two biphasic liquid ⇆ vapor domains,

- one monophasic vapor domain.

Due to the immiscibility in the liquid phase, a heteroazeotropic invariant was observed, involving three phases in equilibrium: L_1+L_2 ⇆ V_H.

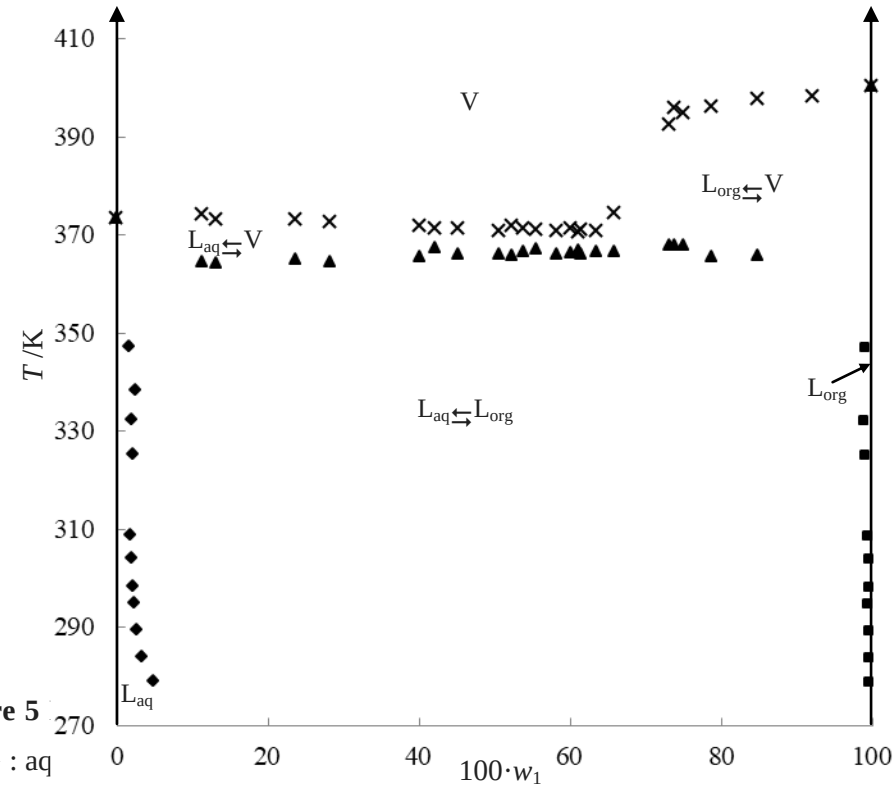

Figure 5 ary system, p = 101.33 kPa ◆ : aq

4. DISCUSSION, MODELLING

4.1. Determination of the heteroazeotrope invariant coordinates

Calorimetric analyses were used to measure the average temperature of the heteroazeotrope: T_H = 366.3 ± 0.6 K. However, they don't give access to the compositions of the three phases in equilibrium: L_1, L_2 and V_H. It is therefore not possible at this stage to represent the two dew curves on the diagram. Since the solubility limits in the liquid phase varied very slightly when approaching the invariant plateau, these mean values were extrapolated to the T_H temperature, which gave the following compositions (Table 6):

Table 6. Molar (*x*) and Mass (*w*) Fractions of the two invariant Liquid phases of the VLL {TMTZ (1) + H_2O (2)} binary mixtures, extrapolated at the T_H Temperature

$T = T_H$	L_1	L_2

$100 \cdot w_1$[a]	2.2	99.3
x_1[a]	0.003	0.955

[a] Standard uncertainties are: $u(100 \cdot w) = 0.2$ %, $u(x) = 0.002$.

The only unknown from now is the composition of the V_H value. In order to have access to this value, we used the Tamman triangle method [19-20], which enabled to determine precisely the composition of the heteroazeotropic point. Indeed, the more the overall composition of the mixture approaches the composition of the heteroazeotrope, the greater the rate of vaporization via the invariant reaction and hence the higher the enthalpy of the endotherm. Thus, the enthalpy of the first peak will be maximum at the V_H composition. The plot of the two straight lines $\Delta H_1 = f(y)$, with y being the weight percentage of TMTZ for $w < w_{VH}$ and $\Delta H_2 = f(z)$, with z being the weight percentage of TMTZ for $w > w_{VH}$, gave a triangle whose summit leads to V_H composition. For the sake of precision, we have also plotted on the graph the line $\Delta H_3 = \Delta_{vap}H(TMTZ) + [\Delta_{vap}H(H_2O) - \Delta_{vap}H(TMTZ)] \times (1-w_{TMTZ})$ [19-20], which is the total apparent vaporization heat of the binary system. These three lines intersect at the composition of the heteroazeotrope (Figure 6).

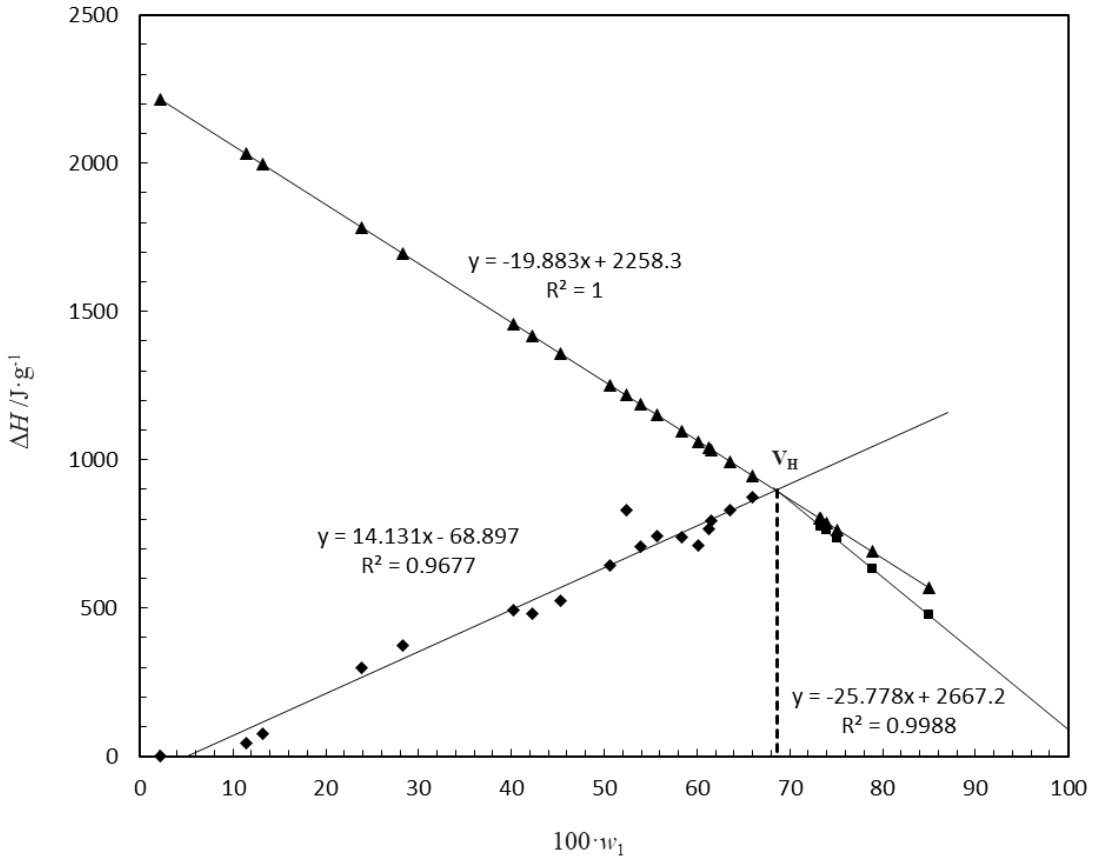

Figure 6 Plot of the Tamman triangles and determination of the heteroazeotrope composition ◆: ΔH_1; ■ : ΔH_2; ▲: ΔH_3

A scattering of the experimental points associated with the straight line ΔH_1 and a loss of precision on the plot of this line was observed. Thus, the corresponding equation was less accurate. This phenomenon is related to the temperature vicinity of the invariant plateau and the dew curve for mixtures with $w < w_{VH}$, which leads to an overlap and a poor deconvolution of the two signals on the corresponding thermograms. Accordingly, it was possible to provide the compositions of the three phases in equilibrium on the heteroazeotropic stage (Table 7):

Table 7. Molar (x) and Mass (w) Fractions of the three phases in equilibrium (L_1, L_2, V_H) at the T_H Temperature of the VLL {TMTZ (1) + H_2O (2)} binary mixtures

$T = T_H$	L_1	L_2	V_H
$100 \cdot w_1$ [a]	2.2	99.3	68.7
x_1 [a]	0.003	0.955	0.254

[a] Standard uncertainties are: $u(100 \cdot w) = 0.2$ %, $u(x) = 0.002$.

The V_H point can now be positioned on the TMTZ + H_2O LV binary diagram, and the dew curves plotted (Figure 7). A discrepancy was observed between the experimental results and the V_H value that was calculated with the Tamman triangles. This is linked to the heteroazeotrope composition uncertainty.

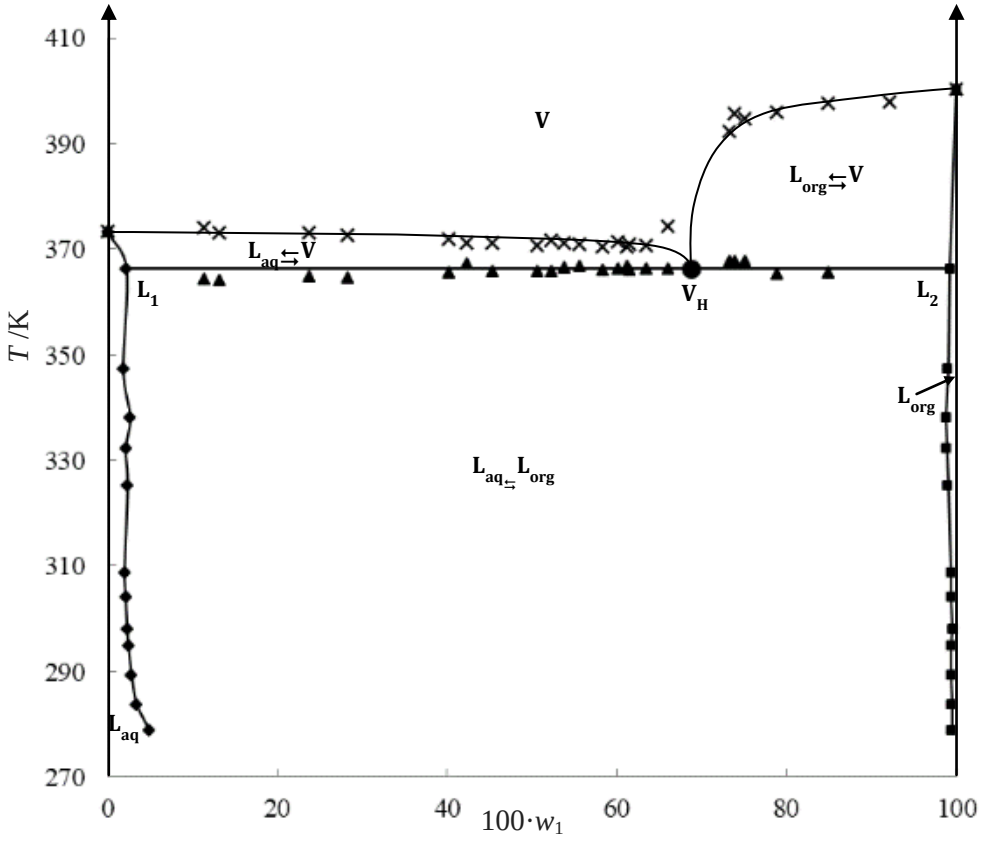

Figure 7 LLV diagram of the {Tetramethyltetrazene (1) + Water (2)} isobar binary system, including all equilibrium curves, p = 101.33 kPa ◆ : aqueous liquid; ■ : organic liquid; ▲: invariant plateau; ×: dew curve

4.2. Thermodynamic modelling of the liquid-vapor equilibria

In general, the starting point of the modelling of phase equilibria relies on the fugacities equality of each constituent between the two phases. In the case of LV equilibria, the following equation can be written: $\bar{f}_i^L(T,p,x) = \bar{f}_i^V(T,p,y)$, in which the subscripts L and V refer respectively to the liquid and vapor phases. The fugacity of a species in the vapor phase can be modeled by an equation-of-state (Virial, Peng-Robinson, Soave-Redlich-Kwong, etc…), or to make it simple, by assuming a mixture of perfect gaseous. To represent the fugacity of a species in the liquid phase, there are two different methods: one based on the activity coefficient models (excess Gibbs energy), and the other, based on the description of the liquid phase by the equations-of-state.

The description of a LV equilibrium using an activity coefficient model for the liquid phase and an equation-of-state for the vapor phase is commonly referred to as the γ-ϕ method (γ = activity coefficient, ϕ = fugacity coefficient) [21]. This method has been chosen for our modelling essays. In the vapor phase, at low pressures and for non-associated compounds, it is usual to consider the mixture as an ideal mixture of perfect gases: $\bar{f}_i^V(T,p,y) = y_{\mathrm{i}} \cdot p$. Liquid phases at low pressures are generally described using the well-known activity coefficient models (Margules, Van Laar, Wilson, NRTL, Uniquac, Unifac, etc…), which are much simpler to use and give very good predictive capabilities. Hence, at low pressures, the equation governing the LV equilibria becomes:

$$x_{\mathrm{i}} \cdot \gamma_{\mathrm{i}}(T,p,x) \cdot p_{s_{\mathrm{i}}}(T) = y_{\mathrm{i}} \cdot p$$

It will then be necessary to use the experimental values for the compositions of the two phases in equilibrium to adjust the parameters of the various models equations that were used for evaluating the activity coefficients. The quantities x_{i} and y_{i} are the experimental molar compositions of component i, respectively in the liquid and vapor phases. γ_{i} is the coefficient of activity of species i as a function of temperature, pressure and composition of the mixture. $p_{s\ \mathrm{i}}$ is the saturating vapor pressure of the pure species i, given generally by Antoine's equations. p is the system's total pressure.

The equations of Antoine (p_s = f (T)) used in our calculations for the two pure compounds are the following: TMTZ: $log\ (p_s) = 9.59 - \frac{1641}{T-46}$ p/Pa, T/K

H_2O [22]: $\log\ (p_s) = 9.65430 - \frac{1435.264}{T-64.848}$ p/Pa, T/K T = (255.8 to 373) K

$\log\ (p_s) = 8.55959 - \frac{643.748}{T-198.043}$ p/Pa, T/K T = (379 to 573) K

As systems containing compounds with strong polarity and structural differences exhibit very limited phenomena of mutual solubility. Hence, calculations have been also carried out to model the demixing curve with these coefficients of activity models.

In this case, the LL equilibrium relation becomes: $x_i^I \cdot \gamma_i^I(T,p,x^I) = x_i^{II} \cdot \gamma_i^{II}(T,p,x^{II})$. Numerous equations have been suggested to model the evolution of the activity coefficients as a function of the molar fraction. In our case, four equations have been tested: Van Laar, Wilson, NRTL (Non Random Two Liquids) and Uniquac (Universal QUAsiChemical). The UNIFAC (UNIversal Functional Activity Coefficient) contribution model, which is purely predictive, has not been studied here because no data regarding the surface and volume group parameters of binary systems containing hydrazines has been found (only the amino, aniline and pyridine groups are tabulated for nitrogen functions) [23]. The behavior of binary systems with quasi-immiscibility in the liquid phase is quite particular, therefore several models have been tested to determine which ones are the most suitable. The purpose of this study is not to detail all the equations of the various models tested, but rather to see their capacity of restitution of the LLV binary system TMTZ + H_2O. It is important to notice that the reported experimental studies on LLV binary systems remain very scarce and those involving hydrazine or tetrazene compounds are non-existent.

Concerning our study, no experimental data on the boiling curve is available (except the boiling temperatures of the pure species and the coordinates of the invariant liquids L_1 and L_2), which are nevertheless very useful, or even indispensable, for adjusting the parameters of the model and running a correlation (the latter being a model based on the activity coefficients therefore by definition, characteristic of the liquid). As a result, it turned out to be difficult to have relevant and optimal modelling, nevertheless the various existing equations have been tested and the parameters have been determined for each model.

The optimized parameters for each equation used are summarized in Table 8.

Table 8. Optimized values of each parameter for the modelling of the VL and LL Equilibria of the {TMTZ (1) + H_2O (2)} binary mixtures

	VLE			LLE	
VAN LAAR	α = 2.8	β = 1.3		α = 5.55	β = 3.33
WILSON	Λ_{12} = 0.01	Λ_{21} = 0.4			
NRTL	α_{12} = 0.47	τ_{21} = 2.8	τ_{12} = 1.1		

In the case of the LL Equilibria, it is important to mention that Wilson equation cannot be applied to systems with partial miscibility. On the other hand, for the studied system, NRTL model did not give relevant results as high deviations were observed between experimental and calculated data. As for the Van Laar equation, no single set of parameters, covering all the temperature range of LL and VL Equilibria, was found. These difficulties of modelling could be linked to the vertical trend of the demixing curves.

The coordinates of the vapor composition of the heteroazeotropic invariant, calculated by the various equations, are depicted in Table 9.

Table 9. Comparison of the experimental and modelled Heteroazeotrope coordinates of the VLL {TMTZ (1) + H_2O (2)} binary mixtures

Model	x_1 [a] VH	T_H [a] /K
VAN LAAR	0.200	368.8
WILSON	0.218	367.4
NRTL	0.213	367.7
Experiments	0.254	366.3

[a] Standard uncertainties are: $u(x_1)$ = 0.002, $u(T)$ = 0.6 K.

4.2.1. Van Laar model

The Van Laar equation is an empirical model of activity coefficient calculation, based on the adjustment of experimental results. It is therefore more a correlative than a predictive model. The two adjustment parameters α and β, corresponding to the calculation of the VL equilibrium curves, are given in Table 7. Moreover, the experimental compositions of the two equilibrium liquids in the demixing zone enabled to adjust another pair of parameters α and β, to calculate the LL equilibria in this zone (Table 7). The results thus obtained are shown in Figure 8.

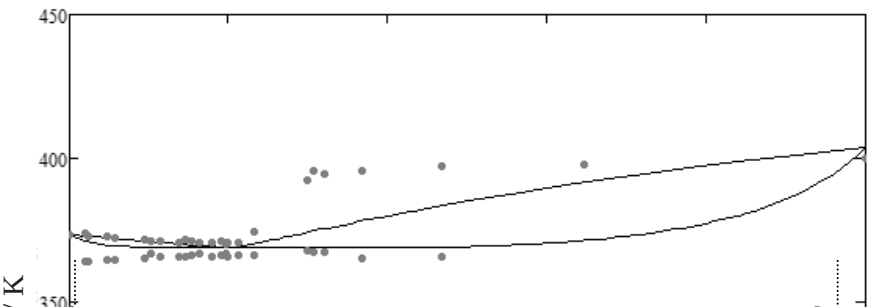

Figure 8 LLV diagram of the {Tetramethyltetrazene (1) + Water (2)} isobar binary system, p = 101.33 kPa •: this work ; – and ···: calculated curves by the Van Laar model

The global appearance of the calculated diagram remains consistent with the experiments. However, the fitting of the Van Laar model shows to be limited, especially in the restitution of behaviors in domains with very low solubility near the pure species and in the right part of the dew curve, a domain corresponding to a vapor in equilibrium with a very rich in TMTZ liquid. The calculated coordinates of the heteroazeotrope seem to be consistent with the dew curve and remain close to the experiments (to be nuanced by considering the scattering of the experimental results).

The deviations between the experimental and fitted results for LV data are gathered in Table 10. For the LL calculated data, the compositions obtained were constant whatever was the temperature: mean deviation from the fit is around 10 % for the aqueous phase (very low concentrations, so, very sensitive to small deviations) and around 1 % for the organic phase.

Table 10. Comparison of the experimental and calculated VLL data in the case of the Van Laar Model for the VLL {TMTZ (1) + H_2O (2)} binary mixtures [Relative deviation $\Delta \boldsymbol{T} = \left|(\boldsymbol{T}_{\mathbf{calc}} - \boldsymbol{T}_{\mathbf{exp}})/\boldsymbol{T}_{\mathbf{exp}}\right|$]

x_1[a]	T_H[a] exp /K	T_H calc /K	ΔT_H /K	T_{vap}[a] exp /K	T_{vap} calc /K	ΔT_{vap} /K
0.000	-	-	-	373.1	373.6	0.001
0.020	364.3	371.4	0.019	374.0	373.4	0.002
0.023	364.0	371.1	0.020	373.0	373.2	0.001

0.046	364.7	369.9	0.014	372.9	372.9	0.000
0.058	364.4	369.6	0.014	372.4	372.4	0.000
0.095	365.4	369.0	0.010	371.7	371.6	0.000
0.102	367.1	369.0	0.005	371.1	371.3	0.001
0.114	365.8	368.9	0.008	371.1	371.1	0.000
0.138	365.8	368.9	0.008	370.6	370.8	0.001
0.146	365.7	368.8	0.008	371.6	370.6	0.003
0.153	366.4	368.8	0.007	371.0	370.3	0.002
0.163	366.8	368.8	0.005	370.8	370.0	0.002
0.179	366.0	368.8	0.008	370.4	369.8	0.002
0.190	366.2	368.8	0.007	371.2	369.3	0.005
0.197	366.6	368.8	0.006	370.2	369.1	0.003
0.199	366.0	368.8	0.008	370.9	369.0	0.005
0.213	366.3	368.8	0.007	370.5	369.8	0.002
0.232	366.3	368.8	0.007	374.3	370.6	0.010
0.299	367.7	368.8	0.003	392.2	374.2	0.046
0.306	367.6	368.8	0.003	395.5	375.0	0.052
0.320	367.7	368.8	0.003	394.7	375.5	0.049
0.367	365.3	368.8	0.010	395.9	378.4	0.044
0.468	365.5	369.1	0.010	397.5	383.6	0.035
0.646	-	-	-	397.9	386.5	0.029
1.000	-	-	-	400.1	404.0	0.010
$\overline{\Delta T}$			0.009			0.011

[a] Standard uncertainties are: $u(x_1) = 0.002$, $u(T) = 0.6$ K.

4.2.2. Wilson model

The following three models, namely Wilson, NRTL and Uniquac, stem from the concept of local composition. This concept assumes that molecules in a microscopic scale are organized into "cells" in which the local compositions differ, due to short-distance interactions, from the overall composition in the mixture. They are not totally predictive because the binary parameters must be determined from experimental data. The main disadvantage and limitation of the Wilson model lies in the inability of its equation -because of its mathematical structure- to model partial miscibility phenomena and to predict the

existence of two stable liquid phases. Therefore, its restitution capacities have been only tested in the temperature domains above the heteroazeotrope.

The two adjustment parameters Λ_{12} and Λ_{21}, corresponding to the calculation of the LV equilibrium curves are given in Table 8 and the modelled equilibrium curves are shown in Figure 9.

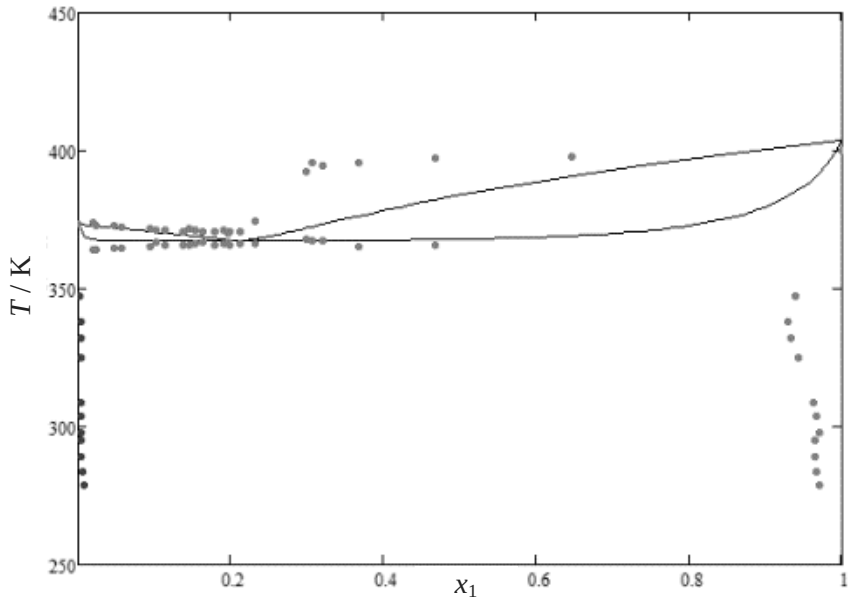

Figure 9 LLV diagram of the {Tetramethyltetrazene (1) + Water (2)} isobar binary system, p = 101.33 kPa •: this work ; –: calculated curves by the Wilson model

It can be noticed that the trend of the modelled curves appears to be very satisfactory, with better fitting results than the Van Laar model, particularly in the restitution of the behavior near the pure compounds and around the heteroazeotropic plateau.

The coordinates of the heteroazeotropic invariant (Table 9) obtained by the various models are very similar and consistent with the plot of the dew curve. It can be underlined that the strong dissimilarity of the two molecules (structure, polarity) induces the non-symmetrical pattern of the diagram and a significant difference of the values obtained for the two adjustment parameters Λ_{12} and Λ_{21}. The model thus remains limited in the restitution of the right part of the dew curve, domain corresponding to a vapor in equilibrium with a very rich in TMTZ liquid. The deviations between the experimental and fitted results are gathered in Table 11.

Table 11. Comparison of the experimental and calculated VLL data in the case of the Wilson Model for the VLL {TMTZ (1) + H_2O (2)} binary mixtures [Relative deviation $\Delta T = |(T_{calc} - T_{exp})/T_{exp}|$]

x_1[a]	T_H[a] exp /K	T_H calc /K	ΔT_H /K	T_{vap}[a] exp /K	T_{vap} calc /K	ΔT_{vap} /K
0.000	-	-	-	373.1	373.6	0.001
0.020	364.3	367.8	0.010	374.0	373.2	0.002
0.023	364.0	367.7	0.010	373.0	372.9	0.000
0.046	364.7	367.5	0.008	372.9	372.4	0.001
0.058	364.4	367.5	0.009	372.4	371.9	0.001
0.095	365.4	367.4	0.005	371.7	371.0	0.002
0.102	367.1	367.4	0.001	371.1	370.5	0.002
0.114	365.8	367.4	0.004	371.1	370.2	0.002
0.137	365.8	367.4	0.004	370.6	369.7	0.002
0.146	365.7	367.4	0.005	371.6	369.4	0.006
0.153	366.4	367.4	0.003	371.0	369.1	0.005
0.163	366.8	367.4	0.002	370.8	368.8	0.005
0.179	366.0	367.4	0.004	370.4	368.3	0.006
0.190	366.2	367.4	0.003	371.2	368.0	0.009
0.197	366.6	367.4	0.002	370.2	367.8	0.006
0.199	366.0	367.4	0.004	370.9	367.4	0.009
0.213	366.3	367.4	0.003	370.5	367.4	0.008
0.232	366.3	367.4	0.003	374.3	367.9	0.017
0.299	367.7	367.4	0.001	392.2	371.6	0.053
0.306	367.6	367.4	0.001	395.5	372.1	0.059
0.320	367.7	367.4	0.001	394.7	373.2	0.054
0.367	365.3	367.5	0.006	395.9	376.0	0.050
0.468	365.5	367.8	0.006	397.5	382.5	0.038
0.646	-	-	-	397.9	390.7	0.018
1.000	-	-	-	400.1	404.0	0.010
$\overline{\Delta T}$			0.004			0.014

[a] Standard uncertainties are: $u(x_1) = 0.002$, $u(T) = 0.6$ K.

4.2.3. NRTL model (Non Random Two-Liquid)

This model can be applied to highly non-ideal systems, with no restriction on the miscibility of the system. It contains three adjustable parameters, τ_{12}, τ_{21} and α_{12}, and is therefore, in principle, more

suitable to fit to a very wide range of deviation to ideality: it is also a weakness because their simultaneous determination requires more experimental data. When experimental data are scarce, the value of α_{12} can be arbitrarily fixed. In general, this value ranges between 0.2 and 0.47 and in most cases [24-25], it takes the value of 0.3. In our case, α_{12} = 0.47 is used because this value is advised for binaries containing compounds with very different polarities. The optimization tests of the NRTL parameters in the LL domain did not produce relevant results and therefore they will not be presented here.

The three adjustment parameters, corresponding to the calculation of the LV equilibrium curves, are given in Table 8 and the calculated equilibrium curves are shown in Figure 10. The modelled data are compared to the experimental results in Table 12.

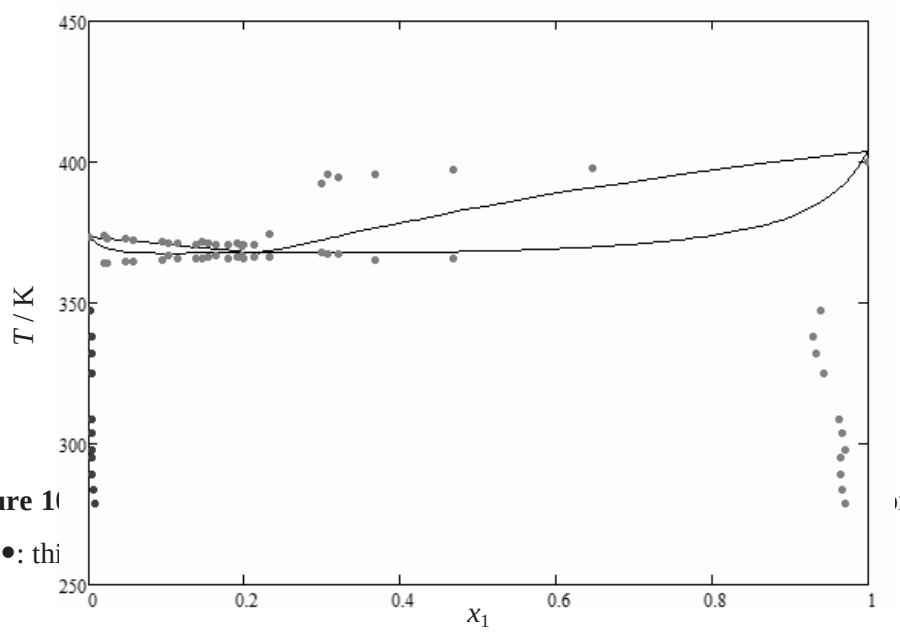

Figure 1( )inary system, p = 101.33 kPa •: thi

Table 12. Comparison of the experimental and calculated VLL data in the case of the NRTL Model for the VLL {TMTZ (1) + H_2O (2)} binary mixtures [Relative deviation $\Delta T = |(T_{calc} - T_{exp})/T_{exp}|$]

x_1[a]	T_H[a] exp /K	T_H calc /K	ΔT_H /K	T_{vap}[a] exp /K	T_{vap} calc /K	ΔT_{vap} /K
0.000	-	-	-	373.1	373.6	0.001
0.020	364.3	369.8	0.015	374.0	373.5	0.001
0.023	364.0	369.5	0.015	373.0	373.0	0.000
0.046	364.7	368.2	0.010	372.9	372.8	0.000
0.058	364.4	367.9	0.010	372.4	372.4	0.000
0.095	365.4	367.7	0.006	371.7	371.4	0.001

0.102	367.1	367.7	0.002	371.1	370.9	0.001
0.114	365.8	367.7	0.005	371.1	370.7	0.001
0.137	365.8	367.7	0.005	370.6	370.0	0.002
0.146	365.7	367.7	0.005	371.6	369.5	0.006
0.153	366.4	367.7	0.004	371.0	369.3	0.005
0.163	366.8	367.7	0.002	370.8	369.1	0.005
0.179	366.0	367.7	0.005	370.4	368.8	0.004
0.190	366.2	367.7	0.004	371.2	368.4	0.008
0.197	366.6	367.7	0.003	370.2	368.1	0.006
0.199	366.0	367.7	0.005	370.9	367.9	0.008
0.213	366.3	367.7	0.004	370.5	367.7	0.008
0.232	366.3	367.7	0.004	374.3	368.1	0.017
0.299	367.7	367.7	0.000	392.2	371.9	0.052
0.306	367.6	367.7	0.000	395.5	372.3	0.059
0.320	367.7	367.7	0.000	394.7	373.1	0.055
0.367	365.3	367.8	0.007	395.9	375.6	0.051
0.468	365.5	368.1	0.007	397.5	380.8	0.042
0.646	-	-	-	397.9	388.8	0.023
1.000	-	-	-	400.1	404.0	0.010
$\overline{\Delta T}$			0.005			0.014

[a] Standard uncertainties are: $u(x_1) = 0.002$, $u(T) = 0.6$ K.

The results are very similar for the three tested models: the diagrams obtained by modelling present the same appearance, as well as the same coordinates calculated for the invariant.

4.2.4. Uniquac model (Universal Quasi-Chemical Theory)

This model relies on the adjustment of two binary interaction parameters, τ_{12} and τ_{21}. It can be applied to highly non-ideal systems with partially miscible behaviors and molecules of very different sizes (due to the decomposition of the equation into a combinatorial and residual part).

However, the optimization of the parameters of this model proved to be very difficult and could not lead to a conclusive and exploitable results for the following reasons:

- no experimental data available for the composition of the liquid in equilibrium in the two-phase LV domains,

- no data referenced in literature tables on volumetric and surface parameters of hydrazine groups (only the data for amine, aniline and pyridine molecules exist),
- since the parameters q_{TMTZ} and r_{TMTZ} are not known, it is necessary to adjust four parameters (q_{TMTZ}, r_{TMTZ}, τ_{12} and τ_{21}) and no longer two. This procedure was attempted but proved to be unsuccessful.

Attempts were also conducted to deduce, by group contribution methods [23,26], the *r* and *q* parameters, characteristics of the TMTZ molecule. However, the obtained values, coupled with the adjustment of the two binary parameters, did not lead to a calculated diagram consistent with the experiments.

In conclusion, this study of the LLV Equilibria of the TMTZ + H_2O system enabled to determine all the parameters defining these equilibria, by combining experimental methods (ebulliometry, DSC) and modelling.

5. CONCLUSION

The VLL TMTZ + H_2O binary system was studied using two experimental techniques (Ebulliometry and DSC), which allowed for the different equilibrium domains to be characterized. The DSC study was focused on the determination of the optimal conditions for observing the vaporization phenomena, which enabled the characterization of the heteroazeotrope and the determination of its coordinates. Besides, the modelling of this binary system by various models (Van Laar, Wilson and NRTL) showed a good consistency between the experimental and the modelled data, and permitted the validation of the experimental DSC method. These data identified the phases in equilibrium as a function of the overall composition and of the temperature. Moreover, the modelled data can be invested for experimental results refining in order to promote the optimization of the various steps involved in the TMTZ extraction process.

ACKNOWLEDGMENTS

This work was supported by Université Claude Bernard Lyon 1, CNRS, CNES and ArianeGroup, which are gratefully acknowledged.

AUTHOR INFORMATION

Corresponding Author

* E-mail: chaza.darwich@univ-lyon1.fr

Tel.: +33472448547

Fax: +33472431291

ORCID

Chaza Darwich: 0000-0003-2332-8132

Notes

The authors declare no competing financial interest.

REFERENCES

[1] Catoire L, Chaumeix N, Pichon S, Paillard C. Visualizations of gas-phase NTO/MMH reactivity. J. Propul. Power. 2006;22(1):120-6.

[2] Frank I, Hammerl A, Klapoetke TM, Nonnenberg C, Zewen H. Processes during the hypergolic ignition between monomethylhydrazine (MMH) and dinitrogen tetroxide (N_2O_4) in rocket engines. Prop., Explos., Pyrotech. 2005;30:44-52.

[3] Nonnenberg C, Frank I, Klapoetke TM. Ultrafast cold reactions in the bipropellant monomethylhydrazine/nitrogen tetroxide: CPMD simulations. Angew. Chem. 2004;43(35):4585-9.

[4] Osmont A, Catoire L, Klapotke TM, Vaghjiani GL, Swihart MT. Thermochemistry of species potentially formed during NTO/MMH hypergolic ignition. Prop., Explos., Pyrotech. 2008;33:209-12.

[5] Sutton GP. History of liquid propellant rocket engines in the united states. J. Propul. Power. 2003;19(6):978-1007.

[6] Schmidt EW. Hydrazine and Its Derivatives: Preparation, Properties, Applications. John Wiley and Sons: New York; 1984.

[7] Carlsen L, Kenesova OA, Batyrbekova SE. A preliminary assessment of the potential environmental and human health impact of unsymmetrical dimethylhydrazine as a result of space activities. Chemosphere. 2007;67:1108-16.

[8] Carlsen L, Kenessov BN, Batyrbekova SY, Kolumbaeva SZ, Shalakhmetova TM. Assessment of the mutagenic effect of 1,1-dimethyl hydrazine. Environ. Toxicol. Pharmacol. 2009;28:448-52.

[9] Choudhary G, Hansen H. Human health perspective on environmental exposure to hydrazines: a review. Chemosphere. 1998;37(5):801-43.

[10] Reddy G, Song J, Mecchi MS, Johnson MS. Genotoxicity assessment of two hypergolic energetic propellant compounds. Mutat. Res. Genet. Toxicol. Environ. Mutagen. 2010;700(1-2):26-31.

[11] Dhenain A, Darwich C, Sabate CM, Le DM, Bougrine AJ, Delalu H, Lacôte E, Payen L, Guitton J, Labarthe E, Jacob G. (E)-1,1,4,4-Tetramethyl-2-tetrazene (TMTZ): a prospective alternative to hydrazines in rocket propulsion. Chem. Eur. J. 2017;23(41):9897-907.

[12] Sabate CM, Delalu H, Guelou Y, Dhenain A, Perut C. Process for preparing alkyltetrazenes. FR2974087A1; 2012.

[13] Mokdad S, Georgin E, Mokbel I, Jose J, Hermier Y, Himbert M. On the way to determination of the vapor-pressure curve of pure water. Int. J. Thermophys. 2012;33(8-9):1374-89.
[14] Mokbel I, Rauzy E, Loiseleur H, Berro C, Jose J. Vapor pressures of 12 alkylcyclohexanes, cyclopentane, butylcyclopentane and trans-decahydronaphthalene down to 0.5 Pa. Experimental results, correlation and prediction by an equation of state. Fluid Phase Equilib. 1995;108(1-2):103-20.
[15] Kasehgari H, Mokbel I, Viton C, Jose J. Vapor pressure of 11 alkylbenzenes in the range 10 – 280 torr, correlation by equation of state. Fluid Phase Equilib. 1993;87(1):133-52.
[16] Kemme HR, Kreps SI. Vapor pressure determination by differential thermal analysis. Anal. Chem. 1969;41(3):1869-72.
[17] Vassallo DA, Harden JC. Precise phase transition measurements of organic materials by differential thermal analysis. Anal. Chem. 1962;34(1):132-3.
[18] Akisawa Silva LY, Matricarde Falleiro RM, Meirelles AJA, Kraehenbuehl MA. Vapor-liquid equilibrium of fatty acid ethyl esters determined using DSC. Thermochim. Acta. 2011;512(1-2):178-82.
[19] Liu ZR, Shao YH. Measurement of the eutectic composition and temperature of energetic materials. Part 1. The phase-diagram of binary systems. Thermochim. Acta. 1995;250(1):65-76.
[20] Yin CM, Liu ZR. Measurement of the eutectic composition and temperature of energetic materials. Part 2. The HX-phase diagram of ternary systems. Thermochim. Acta. 1995;250(1):77-83.
[21] Wong DSH, Sandler SI. A theoretically correct mixing rule for cubic equations of state. AICHE J. 1992;38(5):671-80.
[22] Stull DR. Vapor pressure of pure substances - organic compounds. Ind. Eng. Chem. 1947;39(4):517-40.
[23] Gmehling J. Data bases of the Dortmund Data Bank, UNIFAC Consortium, http://www.ddbst.com/published-parameters-unifac.html#List Of Sub Groups And Their Group Surfaces And Volumes.
[24] Renon H, Prausnitz JM. Local composition in thermodynamic excess functions for liquid mixtures. AICHE J. 1968;14:135-44.
[25] Renon H, Prausnitz J. Estimation of parameters for NRTL equation for excess Gibbs energies of strongly nonideal liquid mixtures. Ind. Eng. Chem. Process Des. Dev. 1969;8(3):413-9.
[26] Bondi A. Van der Waals volums and radii. J. Phys. Chem. 1964;68(3):441-51.

FOR TABLE OF CONTENTS USE ONLY

Title: Measurements of isobaric VLL equilibria of the 1,1,4,4-Tetramethyl-2-tetrazene – Water binary system: novel experimental approach and modelling essays

Authors: Anne-Julie Bougrine, Anne Renault, Marie-Rose Frangieh and Chaza Darwich*